Article

SOURCE DATA | TRANSPARENT PROCESS

THE EMBO JOURNAL

Deletion of PIKfyve alters alveolar macrophage populations and exacerbates allergic inflammation in mice

Takumi Kawasaki[1,*], Kosuke Ito[1], Haruhiko Miyata[2], Shizuo Akira[3,4] & Taro Kawai[1,**]

Abstract

Alveolar macrophages (AMs) are specialized tissue-resident macrophages that orchestrate the immune responses to inhaled pathogens and maintain organ homeostasis of the lung. Dysregulation of AMs is associated with allergic inflammation and asthma. Here, we examined the role of a phosphoinositide kinase PIKfyve in AM development and function. Mice with conditionally deleted PIKfyve in macrophages have altered AM populations. PIKfyve deficiency results in a loss of AKT activation in response to GM-CSF, a cytokine critical for AM development. Upon exposure to house dust mite extract, mutant mice display severe lung inflammation and allergic asthma accompanied by infiltration of eosinophils and lymphoid cells. Moreover, they have defects in production of retinoic acid and fail to support incorporation of Foxp3^{+} T_{reg} cells in the lung, resulting in exacerbation of lung inflammation. Thus, PIKfyve plays a role in preventing excessive lung inflammation through regulating AM function.

Keywords alveolar macrophage; anti-inflammatory response; inositol lipid; lipid kinase; macrophage development

Subject Categories Immunology

DOI 10.15252/embj.201695528 | Received 18 August 2016 | Revised 14 March 2017 | Accepted 7 April 2017 | Published online 22 May 2017

The EMBO Journal (2017) 36: 1707–1718

Introduction

Tissue-resident macrophages are heterogeneous cells that have distinct functions in organ homeostasis and innate immune responses to pathogens. In the lung, alveolar macrophages (AMs) reside in the airway lumen or alveolar space, where they encounter and eliminate inhaled pathogens or dust particles. In addition, AMs play a role in maintenance of surfactant homeostasis, which helps to maintain the air–liquid interface of the alveolar wall to prevent alveolar collapse. Ablation of AMs is known to cause pulmonary alveolar proteinosis (PAP), which is characterized by the accumulation of surfactant material and respiratory insufficiency (Martinez-Moczygemba *et al*, 2008; Suzuki *et al*, 2008). Therefore, AMs play a central role in host defense and in the maintenance of immune and organ homeostasis of the lung (Hussell & Bell, 2014).

The origin of tissue-resident macrophages has long been debated. Recent fate-mapping studies using genetic markers have demonstrated that macrophage populations, including peritoneal, splenic, lung, and liver macrophages, are established from tissue monocytes localized prior to birth, but not from circulating blood monocytes (Yona *et al*, 2013; Ginhoux & Guilliams, 2016). AMs develop from fetal monocytes that adopt a stable phenotype shortly after birth in the lung (Guilliams *et al*, 2013; Schneider *et al*, 2014; Hoeffel *et al*, 2015), although the underlying mechanisms that regulate development and maturation of AMs are not fully understood. Among the various type of tissue-resident macrophages, AMs have distinctive phenotypes that include high autofluorescence, low CD11b expression, and high CD11c and Siglec-F expression (Guilliams *et al*, 2013). Furthermore, localized monocytes in the lung predominantly develop to AM in the presence of GM-CSF (*Csf2*), and therefore, mutations in the *Csf2* and GM-CSF receptor (*Csf2ra* and *Csf2rb*) genes are associated with reduced number and function of AMs, resulting in PAP (Whitsett *et al*, 2010). Similarly, mice lacking *Csf2* and *Csf2rb* develop PAP and display increased susceptibility to bacterial and fungal infection (Paine *et al*, 2001; Yoshida *et al*, 2001; Martinez-Moczygemba *et al*, 2008; Suzuki *et al*, 2008, 2014).

Allergic asthma is a chronic inflammatory disease, which is orchestrated by various types of immune cells, including dendritic cells (DCs), T cells, eosinophils, neutrophils, basophils, innate lymphoid cells (ILCs), and AMs (Galli *et al*, 2008; Lambrecht & Hammad, 2015). Development of allergic asthma is generally controlled by DCs directed toward the adaptive T helper 2 (Th2)-type immune response, which is initially activated by inhaled antigen particles such as house dust mite (HDM), pollen, and fungal spores. These allergic antigens are recognized by pattern-recognition receptors (PRRs) such as Toll-like receptors (TLRs), RIG-I-like receptors (RLRs), C-type lectin receptors, NOD-like receptors, and DNA

1 Laboratory of Molecular Immunobiology, Graduate School of Biological Sciences, Nara Institute of Science and Technology (NAIST), Nara, Japan
2 Department of Experimental Genome Research, Research Institute for Microbial Diseases, Osaka University, Osaka, Japan
3 Department of Host Defense, Research Institute for Microbial Diseases, Osaka University, Osaka, Japan
4 Laboratory of Host Defense, Immunology Frontier Research Center (IFReC), Osaka University, Osaka, Japan
*Corresponding author. Tel: +81 743 72 5550/5532; Fax: +81 743 72 5539; E-mail: kawast01@bs.naist.jp
**Corresponding author. Tel: +81 743 72 5550/5532; Fax: +81 743 72 5539; E-mail: tarokawai@bs.naist.jp

sensors (Kawai & Akira, 2011). HDM contains Der p2 antigen, which displays sequence homology with MD-2, a cell surface molecule bridging LPS to TLR4, and triggers cytokine production and airway allergy by stimulating TLR4 on epithelial cells (Hammad *et al*, 2009). The development of HDM-induced airway allergy in mice is likely to be relevant to human asthma (Gregory *et al*, 2009). AMs have the anti-inflammatory properties of inhibiting DC antigen presentation (Holt *et al*, 1993) and producing immunosuppressive mediators such as IL-10 and nitric oxide (NO) (Martinez *et al*, 1997). These immunological properties suggest that AMs have suppressive roles for asthma development, but the contribution of AMs to asthma has not been clearly demonstrated (Mathie *et al*, 2015).

We previously showed that the phosphatidylinositol lipid PtdIns5P, which is produced by PIKfyve, is involved in innate immune responses to virus infection (Kawasaki *et al*, 2013). PIKfyve is a phosphatidylinositol lipid kinase, which phosphorylates the phosphatidylinositol ring at the 5′ position to produce PtdIns5P or PtdIns3,5P_2. PtdIns5P and PtdIns3,5P_2 are minor phosphatidylinositol lipids that also contribute to diverse cellular functions including vesicular trafficking (McCartney *et al*, 2014), ion channel activation (Li *et al*, 2013), and EGFR signaling (Er *et al*, 2013). It has been reported that PIKfyve-deficient mice are embryonic lethal (Ikonomov *et al*, 2011; Takasuga *et al*, 2013). Using the Cre-loxP system or gene trap mice, the contribution of PIKfyve to various tissue-specific cells such as intestine (Takasuga *et al*, 2013) and platelets (Min *et al*, 2014) was investigated, and PIKfyve was found to play essential roles in cellular development and function.

Here, to investigate the functional role of PIKfyve in macrophages, we generated macrophage-specific PIKfyve-deficient mice. We found that *PIKfyve*$^{flox/flox}$ *lysm-cre* mice have alterations of AMs population. By contrast, the population of tissue-resident macrophages in spleen, liver, bone, or peritoneal cavity was not influenced in *PIKfyve*$^{flox/flox}$ *lysm-cre* mice. Macrophage-specific PIKfyve-deficient mice exhibit an increased severity of inflammation and allergic asthma induced by HDM, which is accompanied by enhanced infiltration of eosinophils and lymphoid cells and production of type 2 cytokines. PIKfyve-deficient mice have defects in retinoic acid induction and fail to recruit T_{reg} cells to the lung. Moreover, AKT activation induced by GM-CSF, a cytokine critical for AM development, was suppressed by PIKfyve deficiency. Thus, PIKfyve is involved in AM development through regulating AKT activation during GM-CSF receptor signaling and is required for prevention from allergic responses to HDM.

Results

Loss of PIKfyve causes a reduction in alveolar macrophage number

To investigate physiological roles of PIKfyve in macrophages, we generated mice lacking PIKfyve in the myeloid lineage. Mice were conditionally targeted with a loxP site flanking exon 5 of the PIKfyve gene (*PIKfyve*$^{flox/flox}$) (Fig EV1A), and *PIKfyve*$^{flox/flox}$ mice were crossed with mice expressing Cre recombinase downstream of the lysozyme LysM promoter (*lysm-cre*). Generation of flox mice was confirmed by Southern blot and PCR analysis (Fig EV1B and C). Immunoblot analysis demonstrated a marked reduction in PIKfyve expression in bone marrow-derived macrophage colony-stimulating factor (M-CSF)-induced macrophages derived from *PIKfyve*$^{flox/flox}$ *lysm-cre* mice (Fig EV1D).

To investigate the function and development of AMs in the lung, bronchoalveolar lavage (BAL) fluid and lung were stained with anti-CD11c and anti-Siglec-F. *PIKfyve*$^{flox/flox}$ *lysm-cre* mice showed reduced numbers of CD11c^{high} and Siglec-F^{high} AMs in both BAL fluid and lung (Fig 1A and B), and reduced expression of the *PIKfyve* gene in AMs (Fig 1C). We next measured various markers in AMs (Fig 1D). AMs from *PIKfyve*$^{flox/flox}$ *lysm-cre* mice had lower autofluorescence (AF), CD64 and CD205 expression, and higher CD86 expression than control cells, but AMs from control and *PIKfyve*$^{flox/flox}$ *lysm-cre* mice did not have significant differences in CD24, IA/IE, Ly-6C, and CD11b expression (Fig 1D), suggesting that AM development is partially retarded in *PIKfyve*$^{flox/flox}$ *lysm-cre* mice.

Lung is known to contain various myeloid lineage cells such as AMs, neutrophils, eosinophils, CD11b$^+$DCs, CD103$^+$DCs, interstitial macrophages (IMs), Ly-6C$^+$ monocytes, and Ly-6C$^-$ monocytes. To characterize these cell populations, we performed 10 color flow cytometry and sequential gating analysis (Misharin *et al*, 2013; Schlitzer *et al*, 2013; Becher *et al*, 2014). After the exclusion of doublet cells, CD45$^+$ cells were stained with antibodies against various cellular surface markers (Fig 2A and B). We first identified CD11b^{int}Siglec-F$^+$ cells and subsequently separated CD11c^{high}CD64$^+$ cells and CD11c$^-$CD64$^-$ cells. CD11b^{int}Siglec-F$^+$CD11c^{high}CD64$^+$ cells were defined as AMs, and CD11c$^-$CD64$^-$Siglec-F$^+$ cells were eosinophils. After segregated neutrophils (CD11b$^+$Ly-6G$^+$) population, CD11c^{high}IA/IE^{high} cells were separated to CD103$^+$DCs (CD11c^{high}IA/IE^{high}CD11b$^-$CD103$^+$) and CD11b$^+$ cells, which were then separated to CD11b$^+$DCs (CD11b$^+$CD24$^+$CD64$^-$) and IMs (CD11b$^+$CD24$^-$CD64$^+$). CD11b$^+$IA/IE$^-$ cells were separated to Ly-6C$^+$ monocytes (CD11b$^+$IA/IE$^-$CD64$^{+/-}$Ly-6C$^+$) and Ly-6C$^-$ monocytes (CD11b$^+$IA/IE$^-$CD64$^-$Ly-6C$^-$). Although populations of these cells were not significantly changed in either control or *PIKfyve*$^{flox/flox}$ *lysm-cre* mice (Fig 2A and B), expression of Siglec-F and CD64 in AMs (CD11b^{int}Siglec-F$^+$CD11c^{high}CD64$^+$) was reduced in *PIKfyve*$^{flox/flox}$ *lysm-cre* mice (Fig 2C), suggesting that *PIKfyve*$^{flox/flox}$ *lysm-cre* mice have altered AM populations. Furthermore, macrophage populations in other tissues, namely spleen, bone marrow, liver, and intraperitoneal fluid, were also investigated by the marker for CD11b and F4/80 (Fig 2D and E). However, these cell populations were comparable in *PIKfyve*$^{flox/flox}$ *lysm-cre* mice.

We also investigated the function of neutrophils isolated from bone marrow. PIKfyve protein expression was reduced in neutrophils (Fig EV2A). The Ly-6C$^+$Ly-6G^{low} monocytes and Ly-6C^{int}Ly-6G^{high} neutrophil populations were unimpaired in *PIKfyve*$^{flox/flox}$ *lysm-cre* mice (Fig EV2B–D). Moreover, IL-6 production after LPS stimulation was normal in *PIKfyve*$^{flox/flox}$ *lysm-cre* mice (Fig EV2E), suggesting that PIKfyve deficiency does not influence both development and function of neutrophils. Taken together, these findings indicate that *PIKfyve*$^{flox/flox}$ *lysm-cre* mice have reduced the number of AMs among various myeloid lineage cells.

PIKfyve deficiency causes alteration in AM populations

Macrophages derived from monocytes have been shown to localize at particular tissues before birth and to mature at the localized tissue

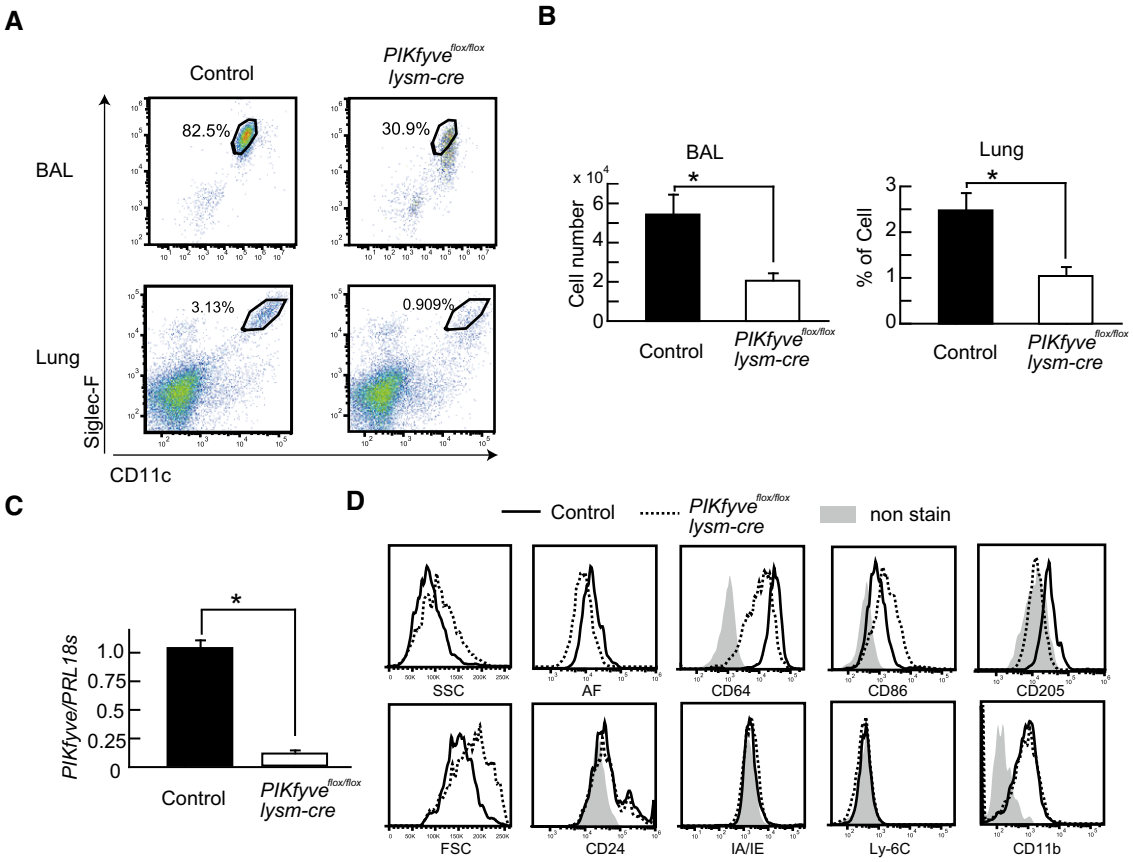

Figure 1. AMs in BAL fluid and lung were reduced in *PIKfyve*$^{flox/flox}$ *lysm-cre* mice.

A Flow cytometry of AMs in BAL fluid and lung stained with anti-CD11c and anti-Siglec-F.

B Number of AMs in BAL fluid and percentage of AMs in lung are shown in bar graphs (n = 4).

C *PIKfyve* gene expression in AMs measured by RT–PCR (n = 3).

D SSC, FSC and autofluorescence (AF), and expression of CD64, CD86, IA/IE, Ly-6C, CD24, CD11b, and CD205 in AMs.

Data information: Data are represented as mean ± SD. *P < 0.05 (Student's t-test).

(Guilliams *et al*, 2013). To address the development of AMs in lung, lungs were isolated at day of birth (DOB), postnatal day 3 (PND3), 3 and 6 weeks and stained with AM markers (Fig 3A). CD45$^+$ blood cells were gated and stained for expression of CD11b and F4/80, and CD11b$^+$F4/80$^+$ myeloid cell populations were then further gated for CD11c and Siglec-F. Most CD11b$^+$F4/80$^+$ myeloid cells were negative for CD11c and Siglec-F at DOB. At PND3, the CD11c^{high}Siglec-F^{int} cell population was greatly increased in both control and *PIKfyve*$^{flox/flox}$ *lysm-cre* mice. At 3 and 6 weeks after DOB, CD11c^{high}Siglec-F^{int} cells displayed increased expression of Siglec-F and developed into CD11c^{high}Siglec-F^{high} cells in control mice, but not in *PIKfyve*$^{flox/flox}$ *lysm-cre* mice (Fig 3A and B). These results suggest that the development of AMs in *PIKfyve*$^{flox/flox}$ *lysm-cre* mice was partially arrested. Therefore, we next investigated whether these cells still have the potential to proliferate. CD11c^{int}Siglec-F^{int} cells or CD11c^{high}Siglec-F^{high} cells in the lung from mice at PND3 or 3 weeks of age, respectively, were stained with DAPI and the cell cycle protein Ki-67 which labels dividing and recently divided daughter cells (Fig 3C and D). Ki-67$^+$DAPI^{low} cells were gated as G_1 stage, and Ki-67$^+$DAPI^{high} cells were gated as SG_2M stage. At PND3, 30% of both control and KO cells were G_1 phase and 5% of cells were SG_2M stage. At 3 weeks after DOB, 12% of control cells and 16% of KO cells were G_1 phase. In addition, 2% of control cells and 3.5% of KO cells were SG_2M stage (Fig 3C and D). These findings indicated that AMs in *PIKfyve*$^{flox/flox}$ *lysm-cre* mice have higher growth potency and were retarded at CD11c^{high}Siglec-F^{int} stage.

Impaired GM-CSF-induced AKT activation in *PIKfyve*$^{flox/flox}$ *lysm-cre* cells

To understand mechanistically why population of AMs is specifically altered among various tissue-resident macrophages in *PIKfyve*$^{flox/flox}$ *lysm-cre* mice, we next examined the expression of PIKfyve by real-time PCR (RT–PCR) and found that *PIKfyve* was expressed almost ubiquitously (Fig 4A). AMs are the only macrophage type known to require GM-CSF for their development from monocytes loaded in the fetal lung (Guilliams *et al*, 2013). We therefore hypothesized that alteration of AMs resulting from PIKfyve deficiency occurred downstream of GM-CSF receptor signaling. To test this, M-CSF-derived bone marrow macrophages were stimulated with GM-CSF for 3 days, and CD11b$^+$F4/80$^+$ macrophages were

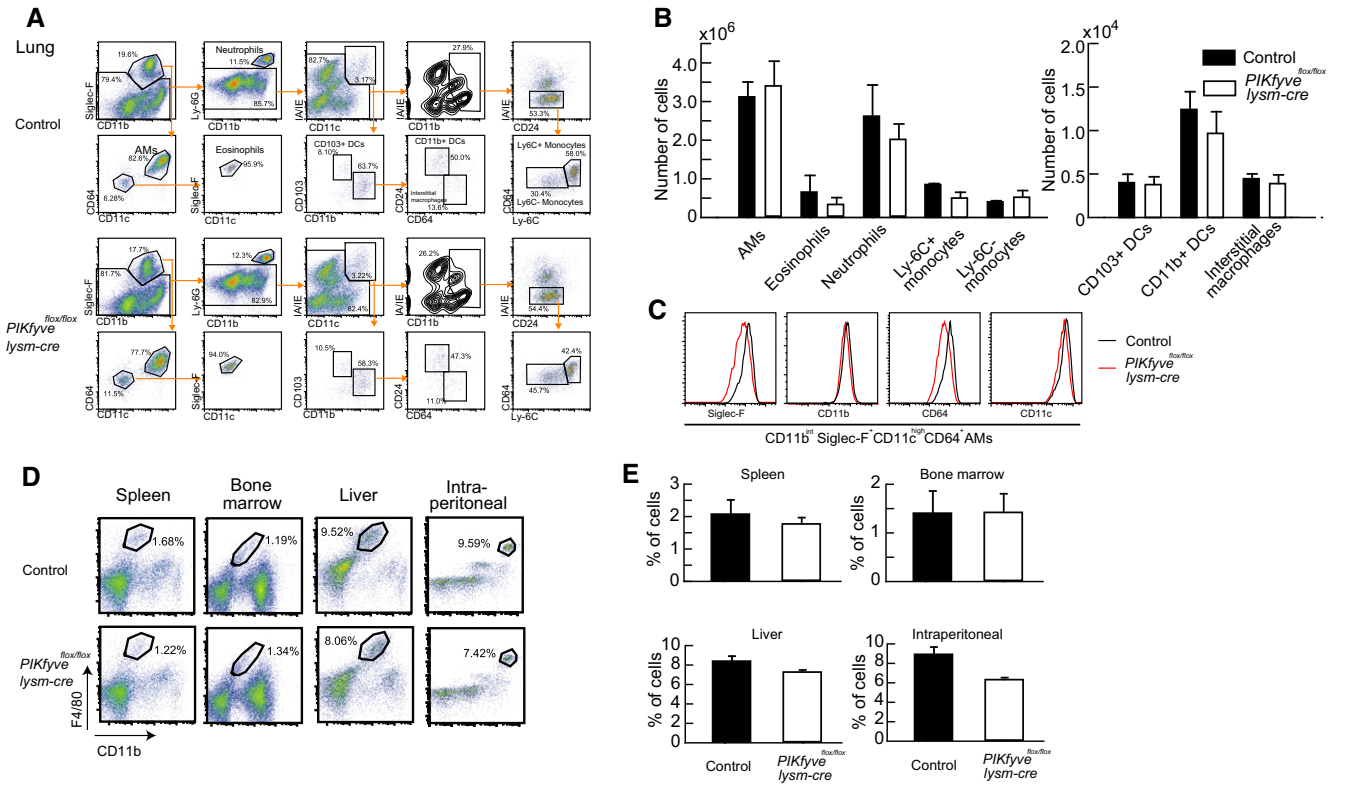

Figure 2. Macrophages and other myeloid linage cell populations in various tissues.

A Gating to separate myeloid lineage cells in lung. Doublet cells were excluded, and CD45$^+$ cells were separated with distinct cell surface markers; alveolar macrophages (AMs) (CD11b^{int}Siglec-F$^+$CD11c^{high}CD64$^+$), eosinophils (CD11c$^-$Siglec-F$^+$), neutrophils (CD11b$^+$Ly-6G$^+$), CD103$^+$ DCs (CD11c^{high}IA/IE^{high}CD11b$^-$CD103$^+$), CD11b$^+$ DCs (CD11c^{high}IA/IE^{high}CD11b$^+$CD103$^-$CD24$^+$CD64$^-$), interstitial macrophages (IMs) (CD11c^{high}IA/IE^{high}CD11b$^+$CD103$^-$CD24$^-$CD64$^+$), Ly-6C$^+$ monocytes (CD11b$^+$IA/IE$^-$CD64$^{+/-}$Ly-6C$^+$), and Ly-6C$^-$ monocytes (CD11b$^+$IA/IE$^-$CD64$^-$Ly-6C$^-$).

B Number of indicated cells in lungs (n = 3).

C Expression of surface makers in CD11b^{int}Siglec-F$^+$CD11c^{high}CD64$^+$ AMs.

D Flow cytometry of spleen, bone marrow, liver, and intraperitoneal cells stained with anti-F4/80 and anti-CD11b.

E Percentage of F4/80$^+$CD11b$^+$ macrophages in each tissue (n = 3).

Data information: Data are represented as mean ± SD.

further stained with anti-CD11c and anti-Siglec-F (Fig 4B). Although the percentages of CD11c$^+$Siglec-F$^+$ cells from control mice and *PIKfyve*$^{flox/flox}$ *lysm-cre* mice were equivalent, percentages of the double-positive cells were increased by GM-CSF stimulation in M-CSF-derived control cells but not in *PIKfyve*$^{flox/flox}$ *lysm-cre* cells (Fig 4B). GM-CSF association with the GM-CSF receptor α and β subunit is known to trigger activation of AKT, STAT5, NF-κB, and MAPK (van de Laar *et al*, 2012). We found that AKT phosphorylation was reduced in M-CSF-induced macrophages from *PIKfyve*$^{flox/flox}$ *lysm-cre* mice relative to control cells (Fig 4C). By contrast, phosphorylation of STAT5, p65 (a subunit of NF-κB), ERK (MAPK), p38, and JNK was comparable in control and *PIKfyve*$^{flox/flox}$ *lysm-cre* cells (Fig 6C). These findings suggest that PIKfyve is required for AKT activation during GM-CSF receptor signaling. Next, expression of ligand and receptor for GM-CSF was investigated in AMs. Expression of the GM-CSF gene *Csf2*, and of the GM-CSF receptor α and β subunit genes *Csf2ra* and *Csf2rb*, was unaltered in AMs or lung tissue in *PIKfyve*$^{flox/flox}$ *lysm-cre* cells (Fig 4D). Surface expression of CD131 (GM-CSF receptor β subunit) was also comparable in AM (Fig 4E). To investigate signaling events in AMs, lungs were isolated at PND3 and CD11c$^+$Siglec-F^{int} cells were stained for pAKT, but pAKT-positive cells were not detectable. At PND5, pAKT-positive cells in CD11c$^+$Siglec-F^{int} cells were increased in control cells but reduced in *PIKfyve*$^{flox/flox}$ *lysm-cre* mice (Fig 4F). By contrast, STAT5 phosphorylation was undetectable in both control and *PIKfyve*$^{flox/flox}$ *lysm-cre* cells (Fig 4G). Gene expression for CD11c^{high}Siglec-F^{high} cells in wild type and CD11c^{high}Siglec-F$^+$ including Siglec-F^{int} cells in *PIKfyve*$^{flox/flox}$ *lysm-cre* mice were compared by gene chip analysis, and several genes were upregulated or downregulated (Fig 4H). Among these, the expression of IRF family genes, encoding transcription factors related to macrophage function and development, was broadly suppressed in *PIKfyve*$^{flox/flox}$ *lysm-cre* cells (Fig 4H). In addition, expressions of signature genes for AM development, of *Pparg*-related genes, or of lipid metabolite genes were broadly dysregulated in *PIKfyve*$^{flox/flox}$ *lysm-cre* mice (Fig EV3A–C). We also investigated gene expression by RT–PCR after separation with Siglec-F^{high} and Siglec-F^{int} cells in *PIKfyve*$^{flox/flox}$ *lysm-cre* mice and found that expression of *PIKfyve*, *Irf8*, and *Irf5* was suppressed in the both cells (Fig EV3D and E). As supported, GM-CSF stimulation increased *Irf8*, *Irf5*, and *Irf1* expression in M-CSF-induced macrophages and expression of these genes was suppressed by the AKT inhibitor (GSK690693)

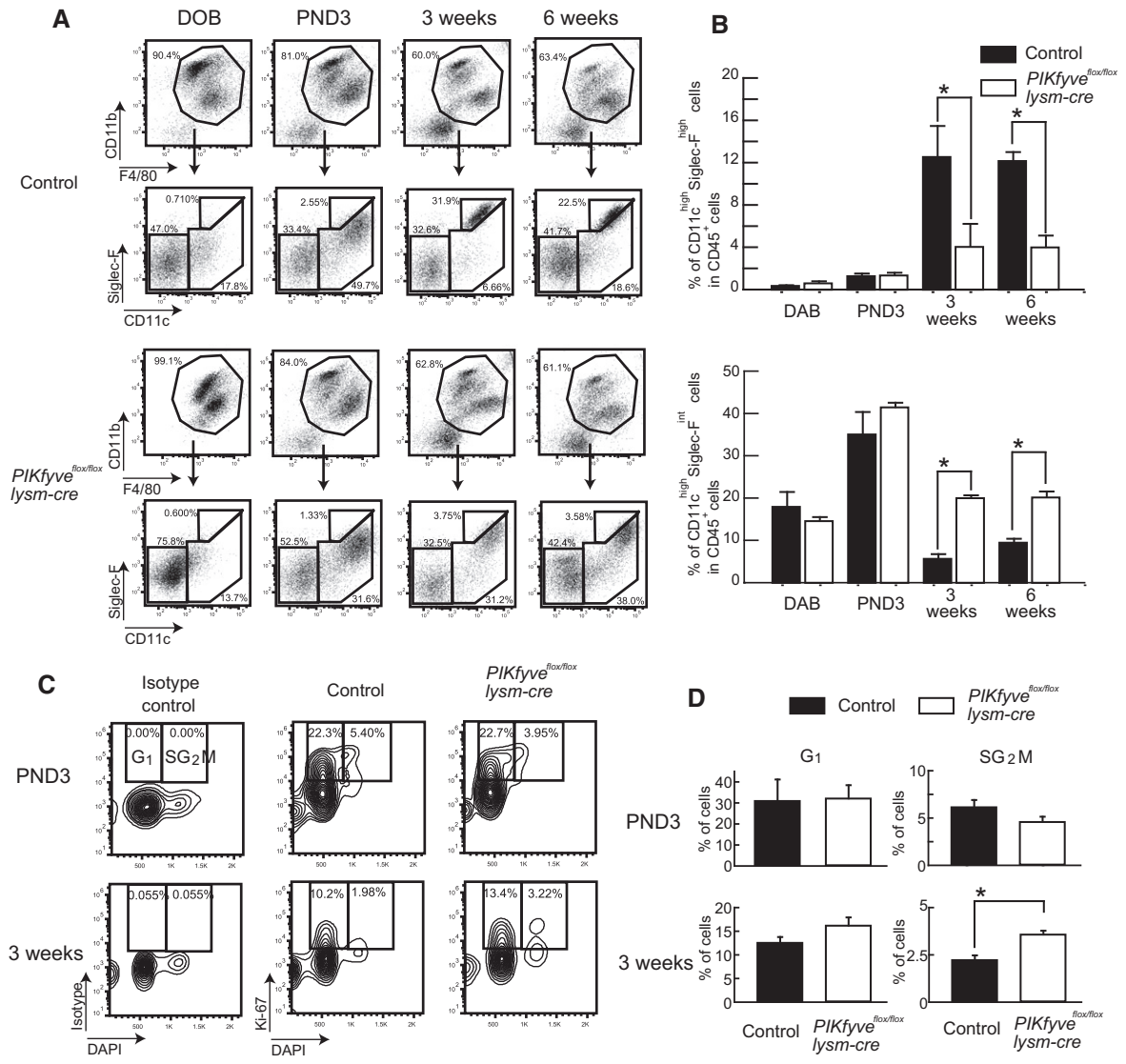

Figure 3. Population of AMs during developmental stages.

A Lungs were harvested at the indicated times after birth and analyzed by flow cytometry. $CD45^+$ blood cells were gated for CD11b and F4/80, and $CD11b^+F4/80^+$ cells were stained with anti-CD11c and anti-Siglec-F.

B Percentages of $CD11c^{high}Siglec\text{-}F^{high}$ AMs (upper) and of $CD11^{high}Siglec\text{-}F^{int}$ AMs (lower) in $CD45^+$ cells are plotted as bar graphs ($n \geq 5$).

C $CD11^{high}Siglec\text{-}F^{high}$ AMs in lung were stained with DAPI and anti-Ki-67 or isotype control. Ki-67^+DAPI^{low} cells were gated as G_1 phase, and Ki-67^+DAPI^{high} cells were gated as SG_2M phase.

D The percentage of G_1 and SG_2M phase cells are plotted as a bar graph ($n = 3$).

Data information: Data are represented as mean ± SD. *$P < 0.05$ (Student's t-test).

(Fig 4I). These results suggest that alteration of AMs in *PIKfyve*$^{flox/flox}$ *lysm-cre* mice is caused by the broad reduction in IRF family genes whose expression is regulated by GM-CSF receptor-AKT signaling axis.

PIKfyve-deficient mice display increased HDM-induced allergic inflammation

Alveolar macrophages play fundamental roles in lung homeostasis by performing phagocytosis of surfactant proteins, and abortion of AMs causes PAP (Suzuki *et al*, 2014). Although AMs in *PIKfyve*$^{flox/flox}$ *lysm-cre* mice show a reduced rate of phagocytosis of OVA proteins (Fig EV4A), expression of surfactant proteins in lung was unimpaired by PIKfyve deficiency and *PIKfyve*$^{flox/flox}$ *lysm-cre* mice did not show PAP-like symptoms (Fig EV4B and C).

Given the association of the allergic response with AMs, mice were challenged with and sensitized by HDM extract derived from *Dermatophagoides pteronyssinus* (Fig 5A). We measured infiltration of neutrophils, eosinophils, and $CD4^+$ T cells in BAL fluid and found that the number of eosinophils and $CD4^+$ T cells increased in HDM-treated *PIKfyve*$^{flox/flox}$ *lysm-cre* mice compared to control mice (Fig 5B). Hematoxylin and eosin (H/E) and periodic

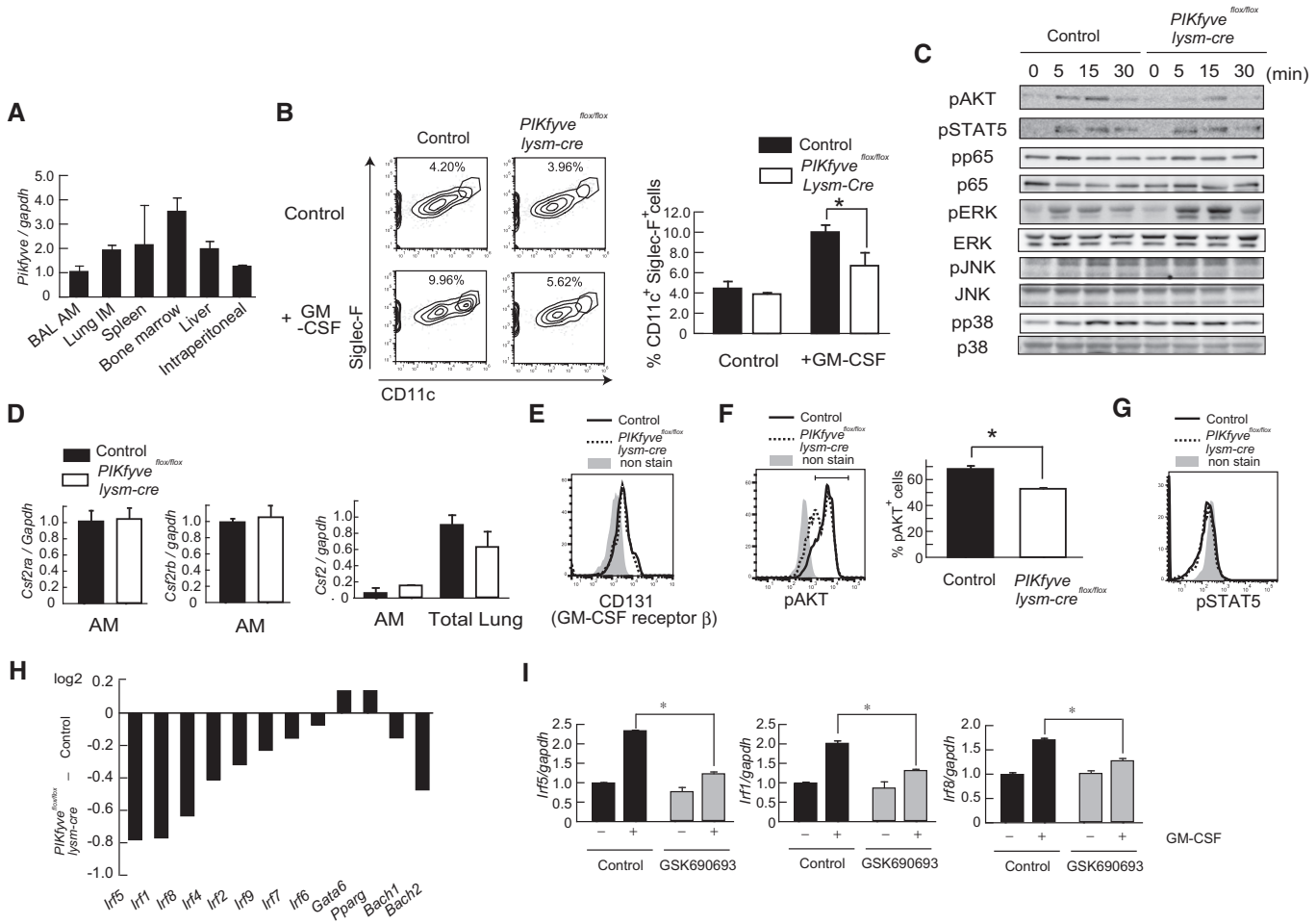

Figure 4. GM-CSF receptor signaling is impaired in *PIKfyve*$^{flox/flox}$ *lysm-cre* mice during AM development.

A AMs and IMs in lung, spleen, bone marrow, liver, and intraperitoneal cavity were isolated, and *PIKfyve* expression was measured by RT–PCR (n = 3).

B M-CSF-induced macrophages were cultured with GM-CSF for 3 days, and CD11b$^+$F4/80$^+$ cells were stained with anti-CD11c and anti-Siglec-F. Percentages of CD11c$^+$Siglec-F$^+$ cells in CD11b$^+$F4/80$^+$ cells are plotted as a bar graph (n = 3).

C M-CSF-induced macrophages were stimulated with GM-CSF, and the time course of phosphorylation level of AKT, STAT5, NF-κB p65, JNK, p38, and ERK was investigated by Western blot analysis using the indicated antibodies.

D AMs or lungs were isolated, and the expression of *Csf2*, *Csfra*, and *Csfrb* was measured by RT–PCR (n = 3).

E Expression of CD131 (GM-CSF receptor β) in AM was measured by FACS (n = 3).

F, G Lungs were isolated at PND5. CD45$^+$ cells were stained with anti-CD11c and anti-Siglec-F, and CD45$^+$CD11c$^+$Siglec-F$^+$ cells were stained with anti-pAKT (F) and anti-pSTAT5 (G). Percentages of pAKT-positive cells are plotted in a bar graph (n = 4).

H CD11c^{high}Siglec-F^{high} cells were isolated from control, and CD11c^{high}Siglec-F$^+$ cells including Siglec-F^{int} cells were isolated from *PIKfyve*$^{flox/flox}$ *lysm-cre* mice. Gene expression in AMs was measured by gene chip analysis, and the expression of transcription factors involved in macrophage development and function is shown.

I M-CSF-induced macrophages were stimulated with GM-CSF in the presence or absence of GSK690693, and the expression of *Irf8*, *Irf5*, and *Irf1* was measured by RT–PCR (n = 4).

Data information: Data are represented as mean ± SD. *P < 0.05 (Student's t-test).
Source data are available online for this figure.

acid Schiff (PAS) staining of lung sections demonstrated that inflammation was exacerbated in HDM-treated *PIKfyve*$^{flox/flox}$ *lysm-cre* mice (Fig 5C). Expression of *Il4*, *Il5*, *Il12*, and *Il13* genes was higher in HDM-treated *PIKfyve*$^{flox/flox}$ *lysm-cre* mice than in control mice, whereas *Il10* expression was not altered (Fig 5D). Production of the Th2-related cytokines IL-4 and IL-13 in lung homogenate was also increased in HDM-treated *PIKfyve*$^{flox/flox}$ *lysm-cre* mice (Fig 5E). It has been reported that HDM-induced allergic inflammation is a Th2-type immune response to which ILCs also contribute synergistically (Lambrecht & Hammad, 2015). Lin$^-$ cells in BAL fluid were further stained by T1/ST2 (IL-1RL1, a subunit of IL-33R) and Sca-1 (Ly-6A/E), and the number of Lin$^-$T1/ST2$^+$Sca1$^+$ ILCs was higher in HDM-treated *PIKfyve*$^{flox/flox}$ *lysm-cre* mice (Fig EV5A and B). *Il33* expression was also increased in lung from *PIKfyve*$^{flox/flox}$ *lysm-cre* mice, but *Tslp* expression was not altered (Fig EV5C). The number of CD11b$^+$ DCs and IMs after HDM treatment was comparable in both control and *PIKfyve*$^{flox/flox}$ *lysm-cre* mice (Fig EV5D and E). These results strongly suggest that allergic

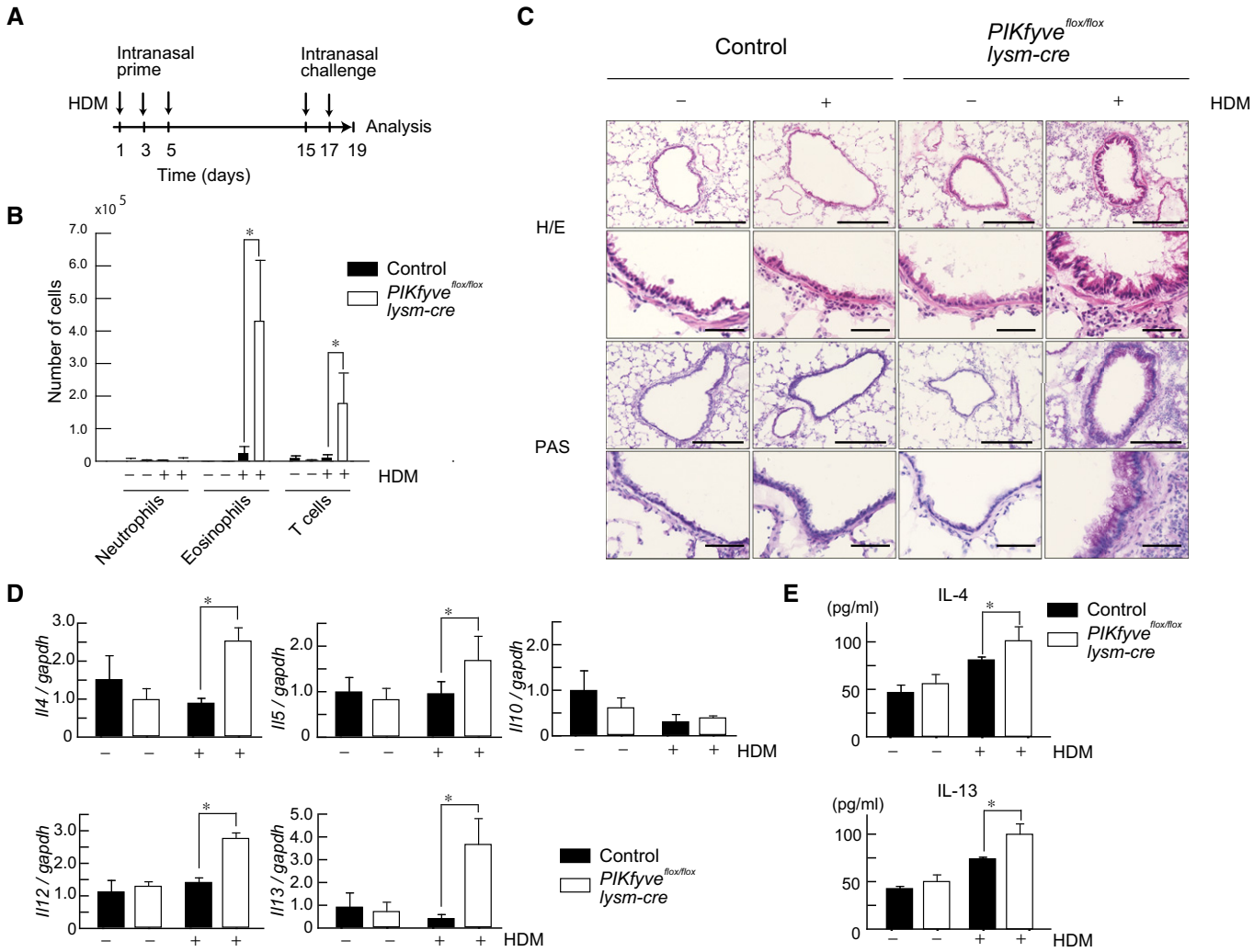

Figure 5. Allergic inflammation in *PIKfyve*$^{flox/flox}$ *lysm-cre* mice is mediated through a Th2-type response.

A Protocol for inducing airway inflammation by HDM intranasal administration.

B Numbers of infiltrating neutrophils, eosinophils, and CD4$^+$ T cells in BAL fluid are plotted as a bar graph (n = 4).

C Representative hematoxylin and eosin (H/E) and periodic acid Schiff (PAS) staining of lung sections. Scale bar: 20 μm (upper) 5 μm (lower).

D Cytokine gene expression in lung tissue was determined by RT–PCR (n = 4).

E Production of IL-4 and IL-13 in lung homogenates was investigated by ELISA (n = 3).

Data information: Data are represented as mean ± SD. *P < 0.05 (Student's t-test).

inflammation in *PIKfyve*$^{flox/flox}$ *lysm-cre* mice is mediated through a Th2-type response.

Egress of allergic asthma in PIKfyve-deficient mice is caused by a reduction in Foxp3$^+$ T$_{reg}$ cells

To investigate whether cells from *PIKfyve*$^{flox/flox}$ *lysm-cre* mice are inflammatory or not, we measured inflammatory cytokines in CD11c^{high}Siglec-F$^+$ cells prepared from mice challenged with HDM (Fig EV6A). Induction of *Tnfa*, *Il6*, and *Il1b* expression was significantly reduced in HDM-challenged PIKfyve-deficient cells, suggesting that CD11c^{high}Siglec-F$^+$ cells from *PIKfyve*$^{flox/flox}$ *lysm-cre* mice are not highly inflammatory. In addition, we measured inflammatory cytokine production by M-CSF-induced bone marrow-derived macrophages (M-BMMs) stimulated with LPS or HDM in the presence or absence of GM-CSF (Fig EV6B). The levels of TNFα, IL-6, and IL-1β after LPS or HDM stimulation were comparable between control and PIKfyve-deficient cells, suggesting that PIKfyve deficiency does not influence macrophage capacities of inflammatory cytokine production in response to LPS or HDM.

Inflammation by Th2 type response is controlled by regulatory T (T$_{reg}$) cells, and T$_{reg}$ cell development is regulated by retinoic acid and TGFβ. Retinoic acid is produced by aldehyde dehydrogenase 1a, which oxidizes retinal and comprises three genes, *Aldh1a1*, *Aldh1a2*, and *Aldh1a3*. Gene expression of *Aldh1a1*, *Aldh1a2*, *Aldh1a3*, and *Tgfb* was measured in AMs in BAL, and in AMs or DCs in lung, by RT–PCR (Fig 6A and B). *Aldh1a1* expression was higher in AMs in BAL, but *Tgfb* was not (Fig 6A). Although *Tgfb*

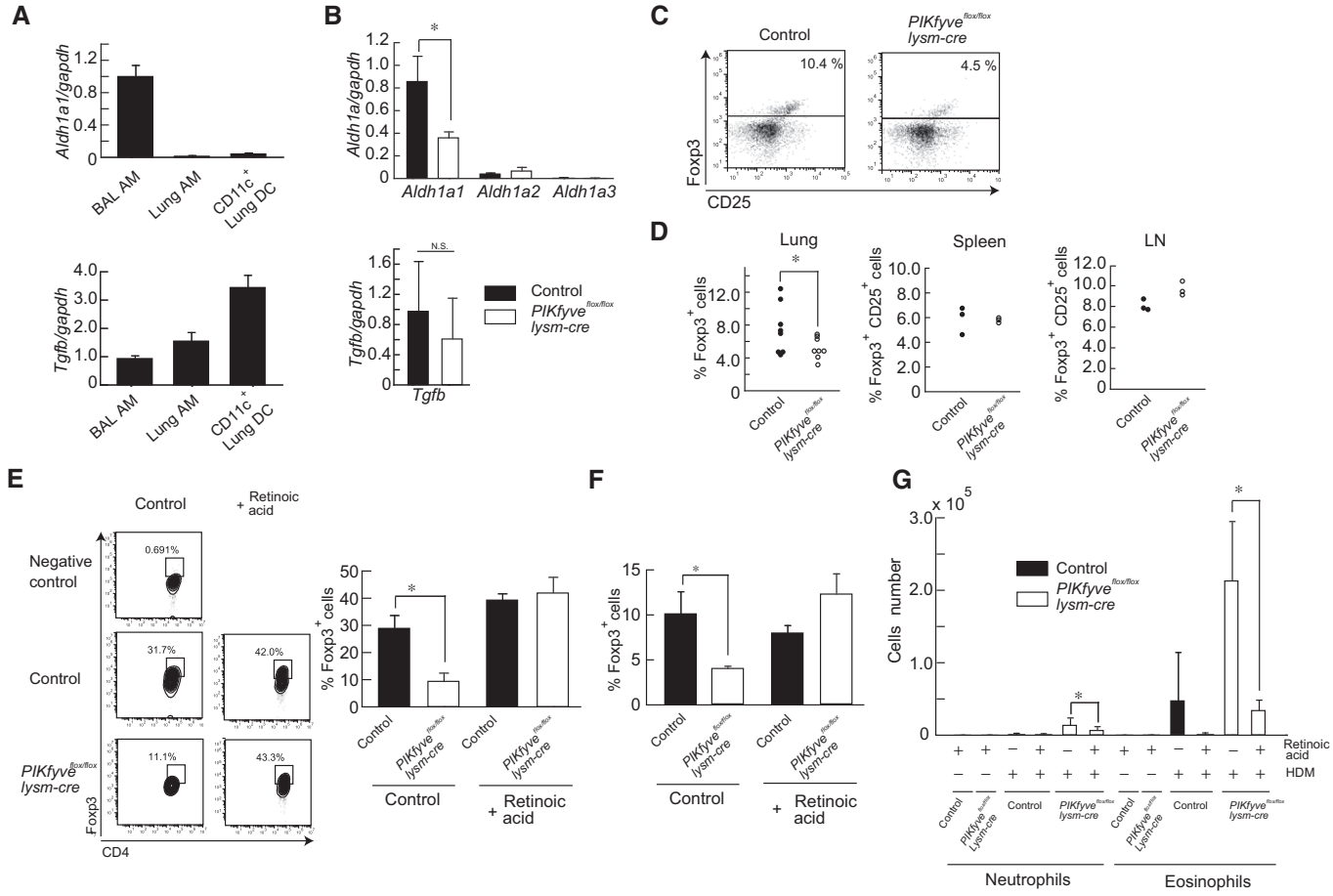

Figure 6. Reduced production of retinoic acid and subsequent failure of Foxp3$^+$ T_{reg} cell incorporation in lung is responsible for exacerbation of HDM-induced allergic inflammation in *PIKfyve$^{flox/flox}$ lysm-cre* mice.

A *Aldh1a1* and *Tgfb* expression in BAL AMs, lung AMs, and CD11c$^+$ DCs was measured by RT–PCR ($n = 3$).

B Comparison of *Aldh1a* and *TGFb* expression in BAL AMs from control and *PIKfyve$^{flox/flox}$ lysm-cre* mice ($n \geq 3$).

C CD4$^+$ T cells in lung were gated for Foxp3 and CD25.

D Percentages of Foxp3-positive T cells in lung, and of Foxp3$^-$ and CD25-positive T cells in spleen and lymph node (LN) are plotted.

E Splenic CD4$^+$CD25$^-$ T cells were isolated and co-cultured with AMs from BAL fluid for 5 days with or without retinoic acid. Total cells were stained with anti-CD4 and anti-Foxp3, and the percentages of Foxp3$^+$ T_{reg} cells in CD4 T cells are plotted as a bar graph ($n = 3$).

F Percentages of Foxp3$^+$ T_{reg} cells in lung after administration of retinoic acid ($n \geq 3$).

G Numbers of neutrophils and eosinophils in BAL fluid after administration of HDM in the presence or absence of retinoic acid ($n \geq 3$).

Data information: Data are represented as mean ± SD. *$P < 0.05$ (Student's *t*-test).

expression was comparable in control and *PIKfyve$^{flox/flox}$ lysm-cre*, *Aldh1a1* expression was higher than *Aldh1a2* and *Aldh1a3* in AMs, and was suppressed in AMs from *PIKfyve$^{flox/flox}$ lysm-cre* mice (Fig 6B), suggesting that T_{reg} cell development is supported by AMs. To examine Foxp3$^+$ T_{reg} cell incorporation in lung, lungs were isolated from HDM-treated mice and stained for CD4, CD25, and Foxp3 (Fig 6C and D). The percentage of Foxp3$^+$ T_{reg} cells in lung was reduced in *PIKfyve$^{flox/flox}$ lysm-cre* mice, whereas CD25$^+$Foxp3$^+$ T_{reg} cells in spleen and lymph node were comparable in both control and *PIKfyve$^{flox/flox}$ lysm-cre* mice (Fig 6C and D). To investigate whether AMs directly regulate Foxp3$^+$ T_{reg} cell development, we used an *in vitro* assay to generate T_{reg} cells from naïve T cells along with AMs. CD4$^+$CD25$^-$ naïve T cells isolated from spleen were cocultured with AMs in BAL from control or *PIKfyve$^{flox/flox}$ lysm-cre* mice (Fig 6E). Foxp3$^+$ T_{reg} cells constituted 30% of CD4$^+$ cells in the presence of AMs from control mice, but only 10% in the presence of AMs from *PIKfyve$^{flox/flox}$ lysm-cre* mice. This reduction in the percentage of Foxp3$^+$ T_{reg} cells by AMs from *PIKfyve$^{flox/flox}$ lysm-cre* mice was rescued by adding retinoic acid to the culture medium. In addition, intranasal administration of retinoic acid rescued the number of T_{reg} cells in *PIKfyve$^{flox/flox}$ lysm-cre* mice (Fig 6F). Consistent with the rescue by retinoic acid of Foxp3$^+$ T_{reg} cell development *in vitro* and *in vivo*, administration of retinoic acid suppressed HDM-induced inflammation in *PIKfyve$^{flox/flox}$ lysm-cre* mice (Figs 6G and EV6C). These results suggest that reduced production of retinoic acid and subsequent failure of Foxp3$^+$ T_{reg} cells incorporation in lung is responsible for exacerbation of HDM-induced allergic inflammation in *PIKfyve$^{flox/flox}$ lysm-cre* mice.

Discussion

Tissue-resident macrophages including AMs are originally derived from fetal monocytes, which are locally loaded before birth and develop to mature macrophages (Guilliams *et al*, 2013). Among the several tissue-resident macrophage types, AMs require GM-CSF for development. In Csf2-deficient mice, early AM commitment from fetal monocytes is impaired. Although short-term perinatal intrapulmonary GM-CSF administration rescues AM development for several weeks, the resulting AMs display immature phenotypes (Guilliams *et al*, 2013). These results suggest that GM-CSF is required at two stages for AM development: early-stage development from fetal monocytes to CD11c^{high}Siglec-F^{int} stage, and late-stage development from CD11c^{high}Siglec-F^{int} to mature CD11c^{high}Siglec-F^{high} stage. The *PIKfyve$^{flox/flox}$ lysm-cre* mice generated in this study show impaired AM development that is retarded at CD11c^{high}Siglec-F^{int} stage (Figs 1 and 2). At DOB, CD11b^{+}F4/80^{+} myeloid cells contain small number of CD11c^{high}Siglec-F^{int} cells, which increased markedly at PND3 in both control and *PIKfyve$^{flox/flox}$ lysm-cre* mice. At 3 and 6 weeks after DOB, CD11c^{high}Siglec-F^{int} cells display an increase in the expression of Siglec-F and develop into CD11c^{high}Siglec-F^{high} cells in control mice, but not in *PIKfyve$^{flox/flox}$ lysm-cre* mice. This finding suggests that AM development in *PIKfyve$^{flox/flox}$ lysm-cre* mice is retarded at the CD11c^{high}Siglec-F^{int} stage that is located at the intermediated stage between fetal monocytes and mature AMs (Fig 3). However, we could not clearly characterize CD11c^{high}Siglec-F^{int} cell population in *PIKfyve$^{flox/flox}$ lysm-cre* mice. Further analyses will be required to determine these cell types.

It is possible that alteration of AM populations in *PIKfyve$^{flox/flox}$ lysm-cre* mice is caused by impaired GM-CSF receptor signaling. Whereas expression of *Csf2*, *Csf2ra*, *Csf2rb*, and CD131 is unimpaired, phosphorylation of AKT, a downstream molecule of GM-CSF receptor signaling, is decreased in AMs from *PIKfyve$^{flox/flox}$ lysm-cre* mice (Fig 4). By contrast, PIKfyve deficiency does not abrogate activation of NF-κB and MAP kinases. These findings suggest that PIKfyve regulates AKT activation during GM-CSF receptor signaling. PIKfyve is a lipid kinase that directly produces PtdIns5P or PtdIns3,5P_2 via phosphorylation of the five position of the inositol ring. A previous study indicated that AKT is activated by PtdIns3,4,5P_3 or PtdIns3,4P_2 (Martelli *et al*, 2006). PIKfyve may indirectly regulate the production of Ptdins3,4,5P_3 or PtdIns3,4P_2, since inositol lipid production is balanced in cells by several kinases and phosphatases. Alternatively, activation of PI3K, which produces Ptdins3,4,5P_3, may be regulated by PIKfyve.

Comparative analysis of transcription factor expression indicated that mRNA expression of the IRF family members was broadly decreased in PIKfyve-deficient AMs (Fig 4H). Whereas PPARγ is a transcription factor that reportedly regulates AM development (Schneider *et al*, 2014), *Pparg* expression was comparable in control and PIKfyve-deficient AMs. AMs in PPARγ-deficient mice show disruption of lipid homeostasis and accumulation of lipid droplets. AMs in PIKfyve-deficient mice, however, showed normal morphology and were not stained with Oil Red O (data not shown). Comparison of expressions of *Pparg*-related genes and lipid metabolite genes suggested that PIKfyve may also be involved in PPAR γ-mediated AM development (Fig EV3B and C). GM-CSF stimulation induced expression of *Irf8*, *Irf5,* and *Irf1* and AKT inhibitor suppressed expression of these genes (Fig 4I). These results indicate that members of the IRF family that are induced by AKT activation during GM-CSF receptor signaling are involved in AM development. Although defective AM development has not been reported, *Irf* genes are required for development and function of various types of myeloid cell linages (Zhao *et al*, 2015). Therefore, it may be possible that multiple IRF family members coordinately regulate AM development. This point should be clarified in the future.

Phagocytosis of surfactant proteins by AMs is crucial for lung homeostasis to prevent PAP disease. Disruption of AMs causes PAP disease, and PPARγ- or Csf2-deficient mice show an accumulation of surfactant proteins and PAP-like symptoms. Phagocytosis of AMs is partially impaired in *PIKfyve$^{flox/flox}$ lysm-cre* mice, but these mice did not develop PAP-like symptoms (Fig EV3). One possible explanation for this relatively minor phenotype in PIKfyve-deficient mice is the expression level of the *cre* gene in AMs. AMs express both LysM and CD11c, and PPARγ deficiency after crossing with *lysm-cre* mice does not lead to a disease phenotype (Gautier *et al*, 2012), whereas PPARγ deficiency after crossing with *CD11c-cre* mice leads to ablation of AMs and progression to PAP-like symptoms (Schneider *et al*, 2014). Therefore, further analysis using PIKfyve$^{flox/flox}$ mice crossed with *CD11c-cre* mice will be required in the future.

PIKfyve ablation causes alteration of AMs population, suggesting the possibility that AM development is arrested at the CD11c^{high}Siglec-F^{int} stage in PIKfyve-deficient mice. PIKfyve-deficient mice are highly sensitive to HDM treatment and show increases in infiltration of eosinophils and lymphoid cells into the BAL space through a Th2-type immune response (Fig 5). Although the contribution of AMs to allergic asthma is controversial (Balhara & Gounni, 2012), our results are consistent with the finding that AM depletion by clodronate liposomes causes egress of HDM-induced asthma (Mathie *et al*, 2015). During the inflammatory response, macrophages switch their phenotype from M1 to M2, which drives the Th2-type immune response (Martinez & Gordon, 2014). However, PIKfyve deficiency did not influence the tendency for M1/M2 polarization (data not shown). In addition, expression of inflammatory cytokines such as *Tnfa*, *Il-6,* and *Il-1b* was unimpaired in PIKfyve-deficient mice (Fig EV6A and B), suggesting that increased allergic responses in PIKfyve-deficient mice are not due to aberrant induction of these inflammatory cytokines. AMs are known to produce TGFβ and retinoic acid, which are likely responsible for induction of Foxp3^{+} T_{reg} cells in the lung (Soroosh *et al*, 2013). The presence of Foxp3^{+} T_{reg} cells inhibits the development of allergic asthma by suppressing the Th2-type immune response (Kim *et al*, 2010; Soroosh *et al*, 2013). Our results suggest that Th2-type immune responses are suppressed by Foxp3^{+} T_{reg} cells that are induced by AMs in control mice, and this suppression is abrogated in *PIKfyve$^{flox/flox}$ lysm-cre* mice. Our results also suggest that premature AMs do not induce sufficient retinoic acid, and therefore, the number of Foxp3^{+} T_{reg} cells in lung is reduced in *PIKfyve$^{flox/flox}$ lysm-cre* mice (Fig 6).

Notably, we found that PIKfyve is dispensable for the population of several tissue-resident macrophage types other than AMs. Although macrophage population in other tissue was unimpaired in PIKfyve-deficient mice, a previous study indicated that not all macrophages are equal in terms of LysM targeting (Schneider *et al*, 2014) and more careful analyses are required to understand the role of PIKfyve in tissue-resident macrophage development. So far, *Csf2*

(Paine *et al*, 2001; Yoshida *et al*, 2001), *Csfrb* (Tanaka *et al*, 2011), *Bach2* (Nakamura *et al*, 2013), and *Pparg* (Schneider *et al*, 2014) have been shown to regulate AM development and function. PIKfyve-deficient mice have altered AM populations and defective AKT activation in response to GM-CSF. PIKfyve-deficient mice are highly sensitive to HDM-induced asthma due to a lack of induction of $Foxp3^+$ T_{reg} cells and increased infiltration of eosinophils and lymphoid cells, suggesting that AM maturation in the lung is a crucial step for preventing asthma following antigen inhalation. We propose that PIKfyve represents a therapeutically important target for the suppression of asthma and lung inflammation in which AMs are involved.

Materials and Methods

Generation of PIKfyve flox mice

PIKfyve-targeted embryonic stem (ES) cells were obtained from the European Mouse Mutant Cell Repository (EuMMCR). The ES cells were generated from JM8/A3, having the C57BL/6 background. Insertion of the targeting cassette at PIKfyve exon 5 was confirmed by Southern blot. ES cells were injected into eight cells stage embryo from ICR female mice, and heterozygous F1 progeny were obtained by crossing with C57BL/6 female mice. F1 mice were crossed with Flp mice to extract the β-geo neomycin cassette. The resultant $PIKfyve^{flox/+}$ mice were crossed with *lysm-cre* mice to generate $PIKfyve^{flox/flox}$ *lysm-cre* mice. All animal maintenance and experiments were performed in accordance with the guidelines of the Committee on Animal Research at Nara Institute of Science and Technology and the Research Institute for Microbial Diseases at Osaka University.

Western blot analysis, cells, and reagents

M-CSF-induced macrophages were obtained from mouse bone marrow cells cultured in RPMI 1640 medium supplemented with 10% heat-inactivated fetal calf serum (FCS, Life Technologies), 100 μM 2-ME, and 10 ng/ml murine M-CSF (ProteoTech) for 5–7 days in a 5% CO_2 atmosphere. Cells were stimulated with 10 ng/ml murine GM-CSF (ProteoTech) and lysed in 25 mM Tris–HCL (pH 8.0), 150 mM NaCl, 10 mM EDTA, 2.5 mM EGTA, 0.2% Triton X-100. Samples were separated by SDS–PAGE and immunoblotted with following antibodies: anti-PIKfyve (P0054) (Sigma), anti-pAKT (17-9715) (eBioscience), anti-pSTAT5 (17-9010) (Cell Signaling), anti-pp65 (#3033S), anti-p65 (#8242S), anti-ERK (#4695P), anti-pERK (#9101S), anti-pp38 (#4511S), anti-p38 (#9212S), and anti-actin (sc-1616) (Santa Cruz Biotechnology). mIL-4 (DY404), mIL-13 (DY413), mTNFα (DY410), mIL-1β (DY401), and mIL-6 (DY406) ELISAs (R&D Systems) were performed according to the manufacturer's instructions. LPS was purchased from Invivogen.

FACS analysis

Bronchoalveolar lavage fluid cells or lung cells were stained with antibody for anti-CD45 (560695, 558702, 560510) (BD Biosciences), anti-CD86 (560582), anti-CD3ε (561108), anti-CD64 (558539), anti-CD4 (553046), anti-CD11c (550261, 562454), anti-Siglec-F (552126), anti-CD24 (560536), anti-Ly-6C (560596), anti-Ly-6G (560600), anti-Sca-1 (553108), anti-CD11b (69-0112) (eBioscience), anti-c-Kit (25-1171), anti-ST2 (17-9335), anti-CD103 (48-1031), anti-CD205 (25-2051), and anti-F4/80 (123128) (BioLegend). Intracellular staining was performed after surface marker staining, and cells were fixed and permeabilized by Transcription Factor Buffer Set (BD Biosciences) and further stained with anti-Foxp3 (12-5773) (eBioscience), anti-Ki-67 (25-5698), anti-pAKT (17-9715), and anti-pSTAT5 (17-9010). Data were collected by FACS Aria or Accuri C6 (BD Biosciences) and analyzed by FlowJo software (TreeStar).

Histological analysis

Lungs were infiltrated with 0.8 ml PBS: O.C.T. Compound (Tissue-Tek), mounted in O.C.T. Compound, and frozen and stored at −80°C. Sections of 10 μm obtained using a cryostat (Thermo Scientific) were collected on glass slides and stained by H/E or PAS.

Quantitative RT–PCR and microarray

Total RNA was isolated using Trizol reagent (Life Technologies) and reverse transcribed by ReverTraAce (Toyobo) according to the manufacturer's instructions. RT–PCR was performed using the following primers: mSPA, sense 5′-taaattgtggccatggaaga-3′, reverse 5′-atgagctgcagaagaagggt-3′; mSPB, sense 5′-ctgcttcctaccctctgc-3′, reverse 5′-cttggcacaggtcattagctc-3′; mSPC, sense 5′-atggacatgagtagca aagaggt-3′, reverse 5′-cacgatgagaaggcgtttgag-3′; mSPD, sense 5′-ca aagggagaacgtggacta-3′, reverse 5′-cttttgcccctgtagatcct-3′; mGAPDH, sense 5′-tgacgtgccgcctggagaaa-3′, reverse 5′-agtgtagcccaagatgccc ttcag-3′; mCsf2ra, sense 5′-cctgctcttctccacgctactg-3′, reverse 5′-gag actcgccggtgtatcc-3′; mCsf2rb, sense 5′-gtggagcgaagagtacacttg-3′, reverse 5′-ccaaagcgaaggatcaggag-3′; mCsf2, sense 5′-acatgacagcca gctactac-3′, reverse 5′-tcaaaggggatatcagtcag-3′; mAldhla1, sense 5′-gacaggctttccagattggctc-3′, reverse 5′-aagactttcccaccattgagtgc-3′; mAldhla2, sense 5′-tggcagaactcagagagtgg-3′, reverse 5′-ccaccttgtc tgcttcttga-3′; mAldhla3, sense 5′-gagcagaaagcaggatgaca-3′, reverse 5′-taaagcatgcgtgtgagtga-3′; mTgfb, sense 5′-caacgccatctatgagaaaa cc-3′, reverse 5′-aagccctgtattccgtctcc-3′; mTslp, sense 5′-tctcaatcctatc cctggct-3′, reverse 5′-cttcttgtgccatttcctga-3′; mIl33, sense 5′-agctggctc tagtggaggag-3′, reverse 5′-ccctttcttcagttggaagc-3′. For microarray analysis, RNA was isolated by spin column (Zymo research) and amplified by OVATION™ RAN amplification system V2. Microarray gene expression data are available from the Gene Expression Omnibus (GEO), accession number GSE93849.

HDM-induced mouse asthma model

Female mice from 8 to 12 weeks of age were intranasally administered 0.2 μg/20 μl DerP1 containing *D. pteronyssinus* extract (Institute of Tokyo Environmental Allergy) at indicated time points, and historical and FACS analyses were then performed.

Statistics

Statistical significance was determined by Student's *t*-test. A *P*-value of < 0.05 was considered significant.

Expanded View for this article is available online.

Acknowledgements

We thank K. Abe for secretarial assistance, and K. Takahashi, A. Takara, and J. Iida for technical support. We also thank NPO for Biotechnology Research and Development for technical assistance. This study was supported by a KAKENHI Grant-in-Aid for Research Activity (C) (26460368; T. Kawasaki), Grant-in-Aid for Research Activity (B) (26293107; T. Kawai), Grant-in-Aid for Scientific Research on Innovative Areas (15H01262; T. Kawasaki and 15H01381; T. Kawai). The study was also supported by the Uehara Memorial Foundation (T. Kawai), the Cell Science Research Foundation (T. Kawai), the Mochida Memorial Foundation for Medical and Pharmaceutical Research (T. Kawai), Takeda Science Foundation (T. Kawai), and the Japan Society for the Promotion of Science through the Funding Program for World-Leading Innovative R&D on Science and Technology (FIRST Program) (S. A.).

Author contributions

TKawas performed experiments, analyzed data, and wrote the manuscript. KI helped with lung sectioning. HM performed ES injection. SA provided material. TKawai wrote the manuscript and supervised research.

Conflict of interest

The authors declare that they have no conflict of interest.

References

Balhara J, Gounni AS (2012) The alveolar macrophages in asthma: a double-edged sword. *Mucosal Immunol* 5: 605 – 609

Becher B, Schlitzer A, Chen J, Mair F, Sumatoh HR, Teng KW, Low D, Ruedl C, Riccardi-Castagnoli P, Poidinger M, Greter M, Ginhoux F, Newell EW (2014) High-dimensional analysis of the murine myeloid cell system. *Nat Immunol* 15: 1181 – 1189

Er EE, Mendoza MC, Mackey AM, Rameh LE, Blenis J (2013) AKT facilitates EGFR trafficking and degradation by phosphorylating and activating PIKfyve. *Sci Signal* 6: ra45

Galli SJ, Tsai M, Piliponsky AM (2008) The development of allergic inflammation. *Nature* 454: 445 – 454

Gautier EL, Chow A, Spanbroek R, Marcelin G, Greter M, Jakubzick C, Bogunovic M, Leboeuf M, van Rooijen N, Habenicht AJ, Merad M, Randolph GJ (2012) Systemic analysis of PPARgamma in mouse macrophage populations reveals marked diversity in expression with critical roles in resolution of inflammation and airway immunity. *J Immunol* 189: 2614 – 2624

Ginhoux F, Guilliams M (2016) Tissue-resident macrophage ontogeny and homeostasis. *Immunity* 44: 439 – 449

Gregory LG, Causton B, Murdoch JR, Mathie SA, O'Donnell V, Thomas CP, Priest FM, Quint DJ, Lloyd CM (2009) Inhaled house dust mite induces pulmonary T helper 2 cytokine production. *Clin Exp Allergy* 39: 1597 – 1610

Guilliams M, De Kleer I, Henri S, Post S, Vanhoutte L, De Prijck S, Deswarte K, Malissen B, Hammad H, Lambrecht BN (2013) Alveolar macrophages develop from fetal monocytes that differentiate into long-lived cells in the first week of life via GM-CSF. *J Exp Med* 210: 1977 – 1992

Hammad H, Chieppa M, Perros F, Willart MA, Germain RN, Lambrecht BN (2009) House dust mite allergen induces asthma via Toll-like receptor 4 triggering of airway structural cells. *Nat Med* 15: 410 – 416

Hoeffel G, Chen J, Lavin Y, Low D, Almeida FF, See P, Beaudin AE, Lum J, Low I, Forsberg EC, Poidinger M, Zolezzi F, Larbi A, Ng LG, Chan JK, Greter M, Becher B, Samokhvalov IM, Merad M, Ginhoux F (2015) C-Myb(+) erythro-myeloid progenitor-derived fetal monocytes give rise to adult tissue-resident macrophages. *Immunity* 42: 665 – 678

Holt PG, Oliver J, Bilyk N, McMenamin C, McMenamin PG, Kraal G, Thepen T (1993) Downregulation of the antigen presenting cell function(s) of pulmonary dendritic cells *in vivo* by resident alveolar macrophages. *J Exp Med* 177: 397 – 407

Hussell T, Bell TJ (2014) Alveolar macrophages: plasticity in a tissue-specific context. *Nat Rev Immunol* 14: 81 – 93

Ikonomov OC, Sbrissa D, Delvecchio K, Xie Y, Jin JP, Rappolee D, Shisheva A (2011) The phosphoinositide kinase PIKfyve is vital in early embryonic development: preimplantation lethality of PIKfyve$^{-/-}$ embryos but normality of PIKfyve$^{+/-}$ mice. *J Biol Chem* 286: 13404 – 13413

Kawai T, Akira S (2011) Toll-like receptors and their crosstalk with other innate receptors in infection and immunity. *Immunity* 34: 637 – 650

Kawasaki T, Takemura N, Standley DM, Akira S, Kawai T (2013) The second messenger phosphatidylinositol-5-phosphate facilitates antiviral innate immune signaling. *Cell Host Microbe* 14: 148 – 158

Kim BS, Kim IK, Park YJ, Kim YS, Kim YJ, Chang WS, Lee YS, Kweon MN, Chung Y, Kang CY (2010) Conversion of Th2 memory cells into Foxp3^{+} regulatory T cells suppressing Th2-mediated allergic asthma. *Proc Natl Acad Sci USA* 107: 8742 – 8747

van de Laar L, Coffer PJ, Woltman AM (2012) Regulation of dendritic cell development by GM-CSF: molecular control and implications for immune homeostasis and therapy. *Blood* 119: 3383 – 3393

Lambrecht BN, Hammad H (2015) The immunology of asthma. *Nat Immunol* 16: 45 – 56

Li X, Wang X, Zhang X, Zhao M, Tsang WL, Zhang Y, Yau RG, Weisman LS, Xu H (2013) Genetically encoded fluorescent probe to visualize intracellular phosphatidylinositol 3,5-bisphosphate localization and dynamics. *Proc Natl Acad Sci USA* 110: 21165 – 21170

Martelli AM, Faenza I, Billi AM, Manzoli L, Evangelisti C, Fala F, Cocco L (2006) Intranuclear 3′-phosphoinositide metabolism and Akt signaling: new mechanisms for tumorigenesis and protection against apoptosis? *Cell Signal* 18: 1101 – 1107

Martinez JA, King TE Jr, Brown K, Jennings CA, Borish L, Mortenson RL, Khan TZ, Bost TW, Riches DW (1997) Increased expression of the interleukin-10 gene by alveolar macrophages in interstitial lung disease. *Am J Physiol* 273: L676 – L683

Martinez FO, Gordon S (2014) The M1 and M2 paradigm of macrophage activation: time for reassessment. *F1000Prime Rep* 6: 13

Martinez-Moczygemba M, Doan ML, Elidemir O, Fan LL, Cheung SW, Lei JT, Moore JP, Tavana G, Lewis LR, Zhu Y, Muzny DM, Gibbs RA, Huston DP (2008) Pulmonary alveolar proteinosis caused by deletion of the GM-CSFRalpha gene in the X chromosome pseudoautosomal region 1. *J Exp Med* 205: 2711 – 2716

Mathie SA, Dixon KL, Walker SA, Tyrrell V, Mondhe M, O'Donnell VB, Gregory LG, Lloyd CM (2015) Alveolar macrophages are sentinels of murine pulmonary homeostasis following inhaled antigen challenge. *Allergy* 70: 80 – 89

McCartney AJ, Zolov SN, Kauffman EJ, Zhang Y, Strunk BS, Weisman LS, Sutton MA (2014) Activity-dependent PI(3,5)P2 synthesis controls AMPA receptor trafficking during synaptic depression. *Proc Natl Acad Sci USA* 111: E4896 – E4905

Min SH, Suzuki A, Stalker TJ, Zhao L, Wang Y, McKennan C, Riese MJ, Guzman JF, Zhang S, Lian L, Joshi R, Meng R, Seeholzer SH, Choi JK, Koretzky G, Marks MS, Abrams CS (2014) Loss of PIKfyve in platelets causes a lysosomal disease leading to inflammation and thrombosis in mice. *Nat Commun* 5: 4691

Misharin AV, Morales-Nebreda L, Mutlu GM, Budinger GR, Perlman H (2013) Flow cytometric analysis of macrophages and dendritic cell subsets in the mouse lung. *Am J Respir Cell Mol Biol* 49: 503 – 510

Nakamura A, Ebina-Shibuya R, Itoh-Nakadai A, Muto A, Shima H, Saigusa D, Aoki J, Ebina M, Nukiwa T, Igarashi K (2013) Transcription repressor Bach2 is required for pulmonary surfactant homeostasis and alveolar macrophage function. *J Exp Med* 210: 2191 – 2204

Paine R III, Morris SB, Jin H, Wilcoxen SE, Phare SM, Moore BB, Coffey MJ, Toews GB (2001) Impaired functional activity of alveolar macrophages from GM-CSF-deficient mice. *Am J Physiol Lung Cell Mol Physiol* 281: L1210 – L1218

Schlitzer A, McGovern N, Teo P, Zelante T, Atarashi K, Low D, Ho AW, See P, Shin A, Wasan PS, Hoeffel G, Malleret B, Heiseke A, Chew S, Jardine L, Purvis HA, Hilkens CM, Tam J, Poidinger M, Stanley ER *et al* (2013) IRF4 transcription factor-dependent $CD11b^+$ dendritic cells in human and mouse control mucosal IL-17 cytokine responses. *Immunity* 38: 970 – 983

Schneider C, Nobs SP, Kurrer M, Rehrauer H, Thiele C, Kopf M (2014) Induction of the nuclear receptor PPAR-gamma by the cytokine GM-CSF is critical for the differentiation of fetal monocytes into alveolar macrophages. *Nat Immunol* 15: 1026 – 1037

Soroosh P, Doherty TA, Duan W, Mehta AK, Choi H, Adams YF, Mikulski Z, Khorram N, Rosenthal P, Broide DH, Croft M (2013) Lung-resident tissue macrophages generate $Foxp3^+$ regulatory T cells and promote airway tolerance. *J Exp Med* 210: 775 – 788

Suzuki T, Sakagami T, Rubin BK, Nogee LM, Wood RE, Zimmerman SL, Smolarek T, Dishop MK, Wert SE, Whitsett JA, Grabowski G, Carey BC, Stevens C, van der Loo JC, Trapnell BC (2008) Familial pulmonary alveolar proteinosis caused by mutations in CSF2RA. *J Exp Med* 205: 2703 – 2710

Suzuki T, Arumugam P, Sakagami T, Lachmann N, Chalk C, Sallese A, Abe S, Trapnell C, Carey B, Moritz T, Malik P, Lutzko C, Wood RE, Trapnell BC (2014) Pulmonary macrophage transplantation therapy. *Nature* 514: 450 – 454

Takasuga S, Horie Y, Sasaki J, Sun-Wada GH, Kawamura N, Iizuka R, Mizuno K, Eguchi S, Kofuji S, Kimura H, Yamazaki M, Horie C, Odanaga E, Sato Y, Chida S, Kontani K, Harada A, Katada T, Suzuki A, Wada Y *et al* (2013) Critical roles of type III phosphatidylinositol phosphate kinase in murine embryonic visceral endoderm and adult intestine. *Proc Natl Acad Sci USA* 110: 1726 – 1731

Tanaka T, Motoi N, Tsuchihashi Y, Tazawa R, Kaneko C, Nei T, Yamamoto T, Hayashi T, Tagawa T, Nagayasu T, Kuribayashi F, Ariyoshi K, Nakata K, Morimoto K (2011) Adult-onset hereditary pulmonary alveolar proteinosis caused by a single-base deletion in CSF2RB. *J Med Genet* 48: 205 – 209

Whitsett JA, Wert SE, Weaver TE (2010) Alveolar surfactant homeostasis and the pathogenesis of pulmonary disease. *Annu Rev Med* 61: 105 – 119

Yona S, Kim KW, Wolf Y, Mildner A, Varol D, Breker M, Strauss-Ayali D, Viukov S, Guilliams M, Misharin A, Hume DA, Perlman H, Malissen B, Zelzer E, Jung S (2013) Fate mapping reveals origins and dynamics of monocytes and tissue macrophages under homeostasis. *Immunity* 38: 79 – 91

Yoshida M, Ikegami M, Reed JA, Chroneos ZC, Whitsett JA (2001) GM-CSF regulates protein and lipid catabolism by alveolar macrophages. *Am J Physiol Lung Cell Mol Physiol* 280: L379 – L386

Zhao GN, Jiang DS, Li H (2015) Interferon regulatory factors: at the crossroads of immunity, metabolism, and disease. *Biochim Biophys Acta* 1852: 365 – 378

